



Short-duration precipitation extremes over Canada in a warmer climate

Seok-Geun Oh¹ · Laxmi Sushama¹

Received: 2 July 2019 / Accepted: 8 January 2020 / Published online: 14 January 2020
© Springer-Verlag GmbH Germany, part of Springer Nature 2020

Abstract

Short-duration precipitation extremes are widely used in the design of engineering infrastructure systems and they also lead to high impact flash flood events and landslides. Better understanding of these events in a changing climate is therefore critical. This study assesses characteristics of short-duration precipitation extremes of 1-, 3-, 6- and 12-h durations in terms of the precipitation-temperature (P–T) relationship in current and future climates for ten Canadian climatic regions using the limited area version of the global environment multiscale (GEM) model. The GEM simulations, driven by ERA-Interim reanalysis and two coupled global climate models (CanESM2 and MPI-ESM), reproduce the general observed regional P–T relationship characteristics in current climate (1981–2010), such as sub-CC (Clausius–Clapeyron) and CC scalings for the coastal and northern, and inland regions, respectively, albeit with some underestimation. Analysis of the transient climate change simulations suggests important shifts and/or extensions of the P–T curve to higher temperature bins in future climate (2071–2100) for RCP4.5 and 8.5 scenarios, particularly for 1-h duration. Analysis of the spatial patterns of dew point depression (temperature minus dew point temperature) and convective available potential energy (CAPE) corresponding to short-duration precipitation extremes for different temperature bins show their changing relative importance from low to high temperature bins. For the low-temperature bins, short-duration precipitation extremes are largely due to high relative humidity, while for high-temperature bins, strong convection due to atmospheric instability brought by surface warming is largely responsible. The analysis thus addresses some of the key knowledge gaps related to the behavior of P–T relationship and associated mechanisms for the Canadian regions.

Keywords Short-duration precipitation extreme · P–T relationship · Climate change · Canada · Global environment multiscale (GEM) model

1 Introduction

In a warmer future climate, the intensity and frequency of extreme precipitation are expected to increase due to the increased water-holding capacity of the atmosphere (e.g., IPCC 2013). Such changes have been reported in various observational and climate modelling studies (e.g., IPCC 2013; Berg et al. 2013), particularly for daily precipitation

extremes. The projection of changes to short-duration such as sub-hourly or sub-daily precipitation extremes is highly desirable for many engineering applications such as storm water drainage and water resource systems. In particular, considering the rapid urbanization that is occurring and the fact that 68% of the population will be living in urban regions by 2050 (United Nations 2017), projected changes to short-duration precipitation extremes that can significantly affect urban infrastructure are essentially required. Regional climate models (RCMs) are useful tools to study projected changes to surface and subsurface climate and hydrological conditions. Indeed, in many socio-economic and engineering fields, RCM-based climate change information is being used to establish effective adaptations to the risks due to global warming. However, RCMs still have difficulty in simulating short-duration precipitation extremes as these extremes are generally mesoscale in nature and are associated with

Electronic supplementary material The online version of this article (<https://doi.org/10.1007/s00382-020-05126-4>) contains supplementary material, which is available to authorized users.

✉ Seok-Geun Oh
seokgeun.oh@mcgill.ca

¹ Department of Civil Engineering and Applied Mechanics and Trottier Institute for Sustainability in Engineering and Design, McGill University, Montreal, Canada

processes such as deep convection, which are not resolved at RCM scales and are represented through various parameterizations. Thus, relatively low-resolution RCMs have substantial biases in simulating short-duration precipitation extremes (e.g., Teufel et al. 2017; Kim et al. 2018; Woodhams et al. 2018; Diro and Sushama 2019).

As an alternative, scaling of short-duration precipitation extremes with respect to temperature increases (P–T relationship, hereafter) is often used to obtain deeper insight on the evolution of extreme precipitation in a changing climate. Precipitation intensities are approximately expected to increase by ~7% per degree warming (°C) according to the Clausius–Clapeyron relationship (CC scaling, hereafter): $de_s/dT = L_v(T)e_s/R_vT^2$ where e_s , T , L_v , and R_v are the saturation vapor pressure, temperature, specific latent heat of evaporation of water, and gas constant of water vapor, respectively. This linear approximation for the saturation-specific humidity is applicable when temperatures are higher than 0 °C and is based on the assumption of constant relative humidity, which would lead to an increase of moisture available to rainstorms at the CC scaling rate (e.g., Shuttleworth 1993; Westra et al. 2014). Lenderink and van Meijgaard (2008), based on their analysis of observed hourly precipitation for summer (JJA) over Netherlands, reported the P–T relationship to be roughly 2 times the CC scaling (super-CC scaling, hereafter) when daily temperature is higher than 12 °C. Furthermore, they confirmed these relations with an RCM-based study for west Europe (Lenderink and van Meijgaard 2010). Following this, studies were carried out for other regions of the world: Europe (Berg et al. 2013; Zhang et al. 2017; Schroeder and Kirchengast 2018), North America (Shaw et al. 2011; Panthou et al. 2014; Prein et al. 2016), and East Asia (Miao et al. 2016; Bao et al. 2017; Park and Min 2017). Most of these studies reported super-CC scaling rates that are substantially larger than 7%/°C for temperatures in the 12–22 °C range, particularly for mid-latitude regions. These studies also noted decrease in precipitation intensities for higher temperatures because of moisture limitation. It must be noted that these studies were conducted on the three assumptions that relative humidity in future climate remains approximately the same as in current climate, the actual precipitation is scaleable to the amount of precipitable water in the atmosphere, and that future atmospheric circulation won't be considerably changed.

Most of the studies over Canada related to short-duration precipitation extremes have focused on trend analysis using observed record (Adamowski et al. 2010; Hogg and Hogg 2010; Shephard et al. 2014) or assessment of future changes based on regional frequency analysis (RFA) approach using an ensemble of RCM simulations (Mladjic et al. 2011; Khaliq et al. 2014). An observation-based study of the P–T relationship was recently performed by Panthou et al. (2014) for seven climatic regions of Canada for the

May–October period. They found that short-duration (5-, 10-, 15-, and 30-min, 1-, and 2-h) precipitation extremes follow CC scaling for the coastal regions, while super-CC scaling was reported for inland regions. These scaling rates were strongly dependent on the precipitation duration and climatic region. The P–T relationship for the inland regions exhibited peak-like structure with precipitation intensities decreasing for higher temperature and reconfirmed that this is related to the change in relative humidity after the breaking point where the highest precipitation intensities occur. Recently, Cannon and Innocenti (2019) using convection-permitting climate model simulations reported significant increases in return levels of short-duration precipitation extremes by late 21st century for North America. In addition, they noted that the rates of 10-year return levels for sub-hourly and sub-daily (1–6 h) durations follow super-CC and CC scalings, respectively. Very few studies have looked at projected changes to the P–T relationship over Canada, in particular focusing on different climatic regions of Canada. This study, therefore, using a state-of-the-art regional climate model, explores the P–T relationship of short-duration precipitation extremes and its projected changes in future climate, related mechanisms and uncertainty across Canadian climatic regions.

The rest of the paper is organized as follows. Section 2 describes the model and methods used in this study. Section 3 evaluates observed and model simulated P–T relationship characteristics for short-duration precipitation extremes for the different climatic regions of Canada, and projected changes to P–T relationship are presented in Sect. 4. Finally, conclusions of this study are presented in Sect. 5.

2 Model and methods

2.1 Model description, data, and study area

The regional climate model used in this study is the limited area version of the global environmental multiscale (GEM) model (Cote et al. 1998; Yeh et al. 2002), which is used for Numerical Weather Prediction by Environment and Climate Change Canada (ECCC). GEM has a non-hydrostatic dynamic core and uses Arakawa C grid staggering in the horizontal and a hybrid terrain-following vertical coordinate. The numerical scheme is a two-time-level, semi-Lagrangian, implicit scheme. The convection schemes of Kain and Fritsch (1992) and Bélair et al. (2005), for deep and shallow convections, respectively, are used. The resolvable large-scale precipitation is calculated following Sundqvist et al. (1989). Radiation is parameterized by the correlated-K solar and terrestrial radiation of Li and Barker (2005). The planetary boundary layer follows Benoit et al. (1989) and Delage (1997), with some modifications as described

in Zadra et al. (2012). The Canadian land-surface scheme (CLASS, Verseghy 2009) version 3.5, allowing a flexible number of layers and depth, is used to represent land processes and lakes are represented by Flake (Martynov et al. 2013).

The model domain used in this study covers North America and adjoining oceans, as shown in Fig. 1. It consists of 212 × 200 grid points (including the blending and halo zones), at 0.44° horizontal resolution and has 56 levels in the vertical. The atmospheric lateral boundary conditions are obtained from the European Centre for Medium-Range Weather Forecast (ECMWF) Re-Analysis (ERA)-Interim data (Dee et al. 2011), the second-generation Canadian Earth System Model (CanESM2, Arora et al. 2011), and the Max Planck Institute for Meteorology Earth System Model (MPI-ESM, Giorgetta et al. 2013). The GEM simulation driven by ERA-Interim for the current 1981–2010

period is used for model evaluation. Two GEM simulations driven by CanESM2 and MPI-ESM for the same 1981–2010 period are also compared with ERA-driven simulation to quantify the uncertainty associated with boundary forcing data. Four GEM simulations driven by CanESM2 and MPI-ESM for RCP4.5 and 8.5 scenarios, are used for the future 2071–2100 period. Hereafter, the GEM simulations driven by ERA-Interim, CanESM2, and MPI-ESM will be referred to as GEM_ERA, GEM_Can, and GEM_MPI, respectively, as shown in Table 1.

The observed hourly precipitation, daily mean surface air temperature, and dew point temperature used to analyze P–T relationship for the current 1981–2010 period are obtained from the observation station networks operated by Environment Canada (Mekis et al. 2018). Periods during which gauging stations are operated vary from year to year and from station to station, but most of the

Fig. 1 Model experimental domain and topography (m), with observation stations indicated by red filled squares. The region enclosed by the inner black box is the free domain. The ten climatic regions considered in this study are also shown: a, WCOAST; b, WCRDRA; c, NWFOR; d, NPLAINS; e, NEFOR; f, MRTMS; g, GRTLKS; h, YUKON; i, MACK; j, EARCT

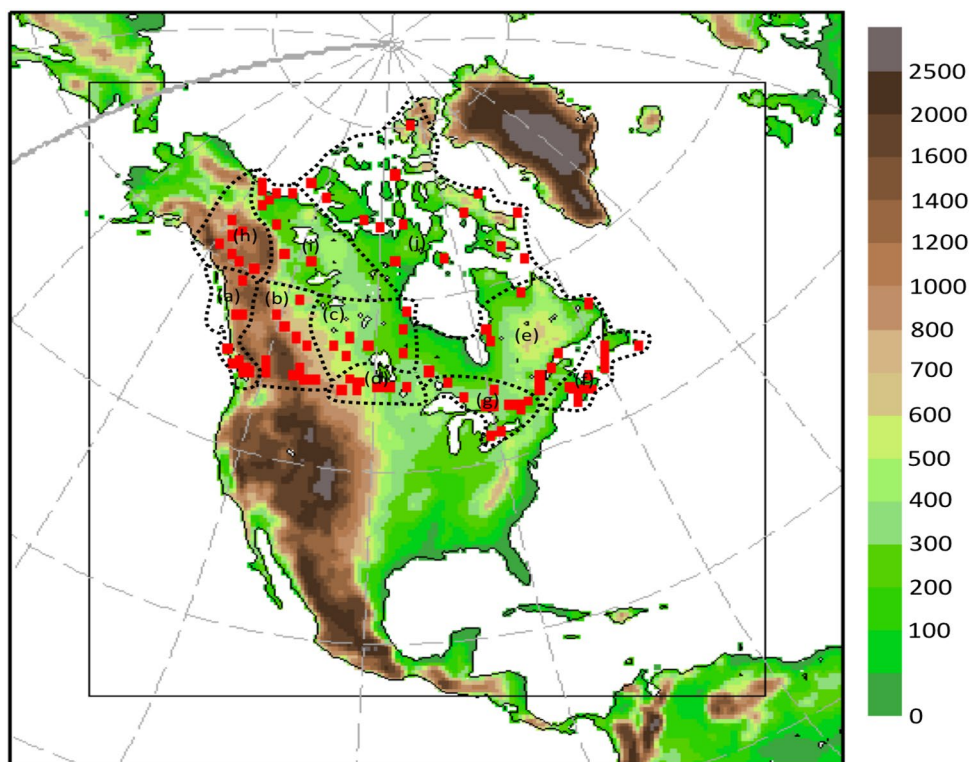


Table 1 The GEM simulations used in this study

Acronym	LBCs	Resolution (Grids: Lon. × Lat.)	Analysis
GEM_ERA	ERA-Interim	0.44° (212 × 200)	May–Oct. 1981–2010
GEM_Can	CanESM2	0.44° (212 × 200)	May–Oct. 1981–2010 May–Oct. 2071–2100 (RCP4.5, RCP8.5)
GEM_MPI	MPI-ESM	0.44° (212 × 200)	May–Oct. 1981–2010 May–Oct. 2071–2100 (RCP4.5, RCP8.5)

The lateral boundary conditions (LBCs) and the analysis periods are also shown

stations are in operation during summer and some in autumn (very few have records during winter). Therefore, the May–October period is considered in this study. 195 observation stations with continuous hourly data for the current 1981–2010 period are considered (Fig. 1). The P–T relationship is evaluated for ten Canadian climatic regions (Fig. 1) defined by Plummer et al. (Plummer 2006). These climatic regions are: West Coast (WCOAST), Western Cordillera (WCRDRA), Northwest Forest (NWFOR), and Northern Plains (NPLAINS), distributed along the western and prairie regions of Canada; Northeast Forest (NEFOR), Canadian Maritimes (MRTMS), and Great Lakes (GRTLKS) in the eastern part of Canada; Yukon Territory (YUKON), Mackenzie Valley (MACK), and East Arctic (EARCT) in the north. For the convenience of analysis and presentation, we further combined these regions into coastal (WCOAST, MRTMS), inland (WCRDRA, NWFOR, NPLAINS, NEFOR, GRTLKS), and northern (YUKON, MACK, EARCT) regions. The observation stations are grouped based on these ten climatic regions (Fig. 1).

2.2 Methods

For P–T relationship analysis, following Lenderink and van Meijgaard (2010), only precipitation intensities larger than 0.3 mm/h are used for the precipitation durations considered in this study, i.e., 1-, 3-, 6-, and 12-h duration. They are classified according to the corresponding daily mean air temperature (or dew point temperature) as follows. The temperature bins are defined by a moving 2 °C window every 1 °C to avoid the choice of odd or even bin limits. For each bin, the reference temperature corresponds to the mean temperature. The distribution of precipitation intensities is then constructed within each temperature bin. The 90th, 95th, and 99th percentiles of precipitation intensities for each temperature bin are calculated for temperature bins with more than 100 values. The model evaluation of P–T relationship is performed by comparing observations with model simulations for the representative grid cell. Climate-change signals are obtained from GEM_Can and GEM_MPI simulations by comparing the future 2071–2100 period with the current 1981–2010 period, for the RCP4.5 and 8.5 scenarios. This study focuses on the climate change assessment for the latter three decades (2071–2100) as the differences between the two analysis periods, scenarios, and simulations are expected to be more distinct in the late 21st century. In addition, it must be noted that the matching current 1981–2010 and future 2071–2100 periods in the GCM-driven simulations are indeed coming from one long simulation spanning the 1950–2100 period.

3 Observed and simulated P–T relationship for the current 1981–2010 period

Figure 2 shows the observed and simulated scaling for the 95th percentile of precipitation intensity with respect to daily mean air temperature and dew point temperature for 1-, 3-, 6-, and 12-h durations for ten climatic regions for the current 1981–2010 period. The precipitation duration and climatic region have a strong influence on the observed P–T relationship. For short durations (1–3 h), the P–T relationship with a peak-like structure, i.e. decreasing precipitation at higher temperatures, is found for the inland regions. The P–T slopes decrease with duration for all regions. The P–T relationship (slopes) for the 90th and 99th percentiles of precipitation intensity are similar to that for the 95th percentile, which means that the P–T slopes are not very sensitive to the percentiles considered here (figure not shown). For the temperature bins between 12 °C and 18 °C for short-durations (1–3 h), super-CC (NPLAINS), CC (WCRDRA, NWFOR, NEFOR, MRTMS, GRTLKS, YUKON, MACK, and EARCT), and sub-CC (WCOAST) scalings are found. This is similar to the findings reported in Panthou et al. (2014). The general features of P–T relationship for all ten climatic regions of Canada are well captured by GEM_ERA simulation. Although the GEM_ERA simulation underestimates the precipitation intensities for all climatic regions, it captures well the CC (NEFOR, NPLAINS, NWFOR, and GRTLKS) and sub-CC scaling (WCRDRA, MRTMS, YUKON, MACK, and EARCT) for short-durations (1–3 h). For the WCOAST, the simulated P–T slopes are close to zero between 0 and 10 °C and show slightly decreasing pattern, as also noticed in observation. These features are similarly captured by the two GCM-driven simulations (see Figures S1 and S2 in the supplementary material). However, relatively more extreme events in temperature bins above 15–20 °C are simulated by GEM_Can, and this is related to the higher rate of warming in GEM_Can compared to GEM_MPI (Diro and Sushama 2017).

Looking at the P–T relationship for the inland regions in detail, the GEM simulations show more distinct peak-like structure than observations and tend to underestimate the breaking point by about 3–5 °C compared to observation. This means that the decrease of the simulated relative humidity starts at lower temperature bins than observed. On the other hand, extreme precipitation events for temperature bins beyond 15 °C are noted in GEM simulations for EARCT, unlike observations. It is related to the warm temperature bias and wet precipitation bias in the GEM simulations for this region during summer (Diro and Sushama 2017; Jeong and Sushama 2018). As shown in Fig. 2b, the observed relationship between extreme

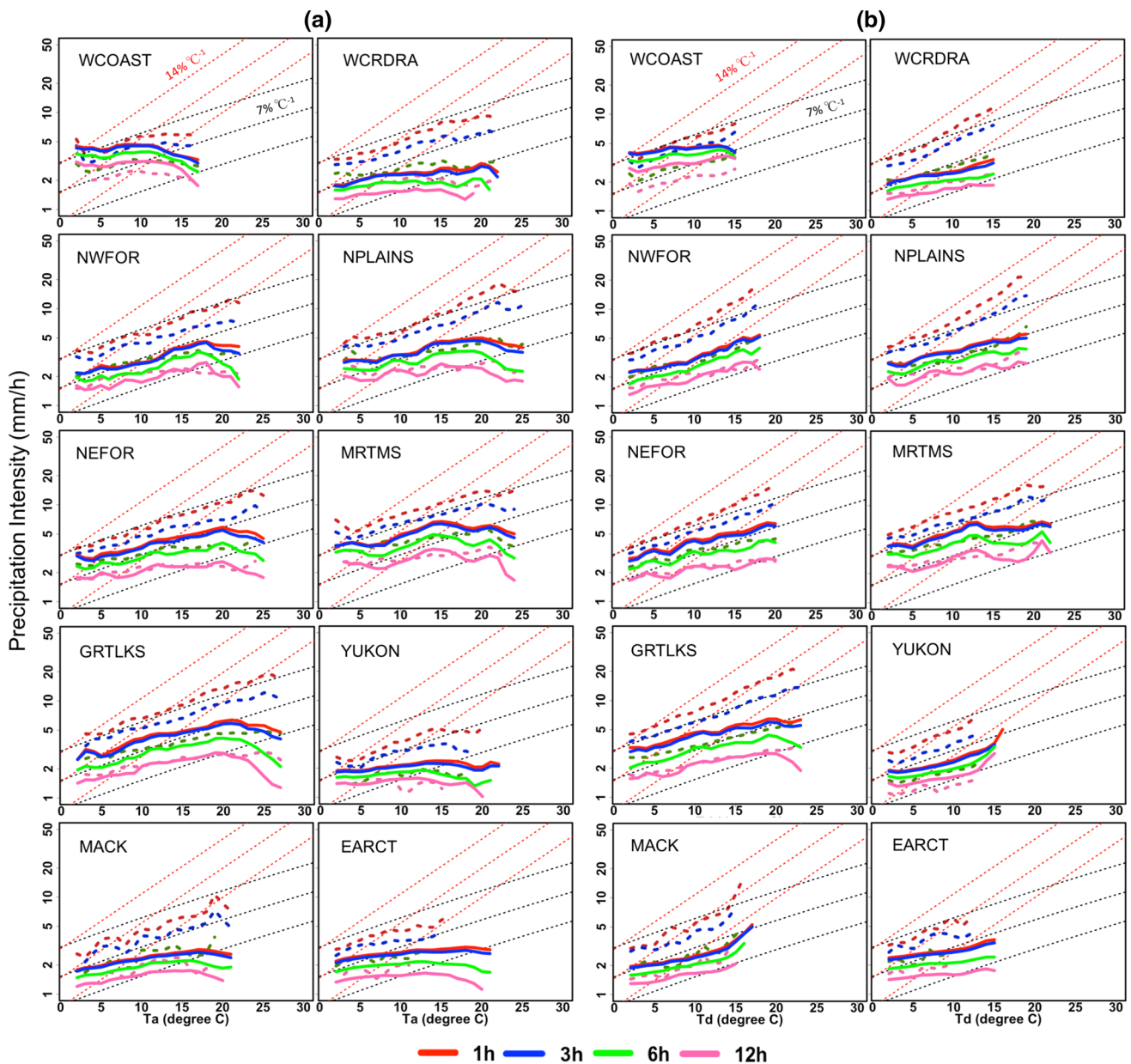


Fig. 2 Observed (dashed lines) and GEM_ERA simulated (solid lines) relationship between the 95th percentile of precipitation intensity and **a** daily mean air temperature (T_a) and **b** dew point tempera-

ture (T_d) for 1-, 3-, 6-, and 12-h durations for the current 1981–2010 period. Black and Red dotted lines correspond to 7%/°C and 14%/°C rates, respectively

precipitation intensities and daily dew point temperature is closer to CC scaling than with daily air temperature, which implies that the P–T slope is primarily linked to the increase in atmospheric moisture with temperature (Lenderink and van Meijgaard 2010), and the GEM simulations well reproduce this feature, regardless of lateral boundary conditions (see Figs. 2, S1, and S2).

Figure 3 shows the observed and simulated spatial pattern of the precipitation scaling rate (%/°C) with respect to daily mean air temperature and dew point temperature for the current 1981–2010 period, which is estimated using a

least squares linear fitting as the change in the 95th percentile of precipitation intensity for 1 h duration up to the breaking point. Sub-CC or CC scaling rates of about 4–6%/°C are observed for inland regions. On the other hand, most of the observations near the coast have relatively low scaling rates of about 1.5–3%/°C (Fig. 3a). These observed scaling rates reveal more robust relationship with dew point temperature and are closer to the CC scaling, in particular for inland regions (Fig. 3b), indicating that the precipitation scaling appears to be primarily linked to the increase in atmospheric moisture with temperature. The general features

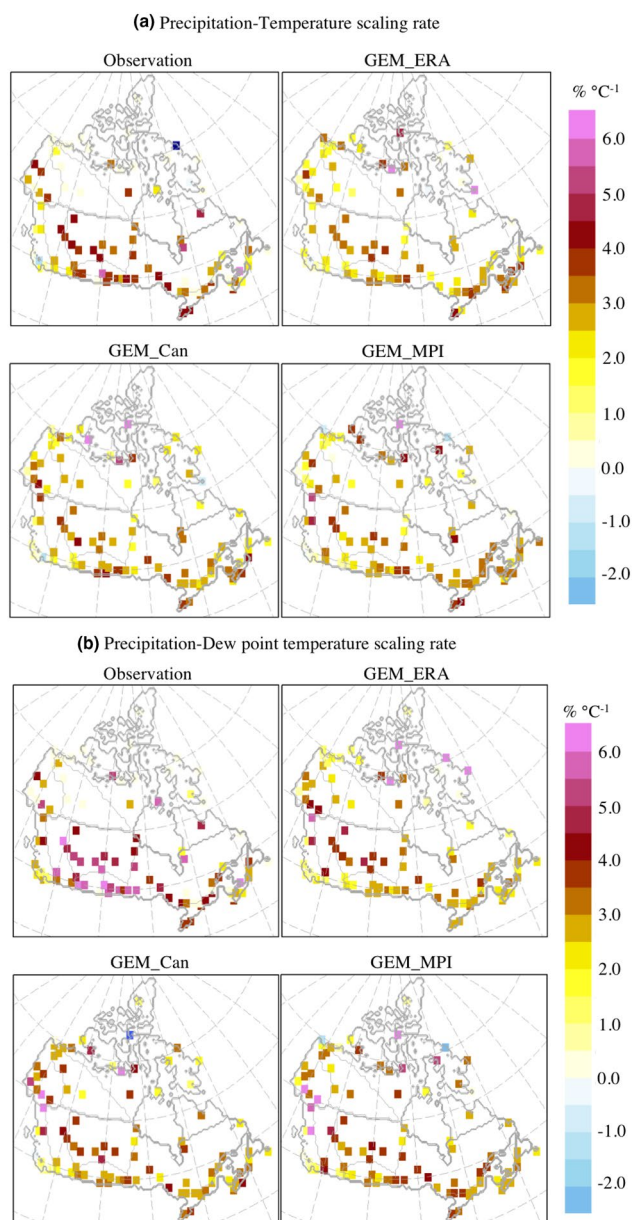


Fig. 3 Precipitation scaling rate ($\%,^{\circ}\text{C}$) with respect to **a** daily mean air temperature and **b** dew point temperature for the current 1981–2010 period, for the 95th percentile of precipitation intensity (mm/h) for 1 h duration

of precipitation scaling depending on the climatic region are also found for other durations considered in this study. For 12 h duration, lower precipitation scaling rates of about $0.5\text{--}1.5/^{\circ}\text{C}$ are observed and some stations within WCOAST suggest negative scaling rates (figure not shown).

The GEM simulations, in general, well reproduce the spatial pattern of the precipitation scaling rates similar to the observation, regardless of the lateral boundary conditions. The precipitation scaling rates, however, are slightly underestimated depending on the observation point, given

the relatively low model resolution and imperfections in the representation of dynamical processes in RCM (e.g., Muller et al. 2011; Romps 2011; Oh and Suh 2018). Robust scaling rates with dew point temperature are reproduced in all GEM simulations, similar to the observations. However, P–T scalings based on the dew point temperature appear more sensitive to the climatic region. Furthermore, noticeable differences between the two GCM-driven simulations are found for the WCOAST, GRTLKS, MRTMS, and YUKON regions, due to the differences in simulated moisture. Given these larger differences in the dew point-based P–T relationship, we focus on projected changes to the P–T relationship based on daily mean air temperature and short-duration precipitation extremes simulated by the GCM-driven GEM simulations.

4 Projected changes to the P–T relationship

The area-averaged scaling of the 95th percentile of precipitation intensity for 1 h duration with respect to daily mean air temperature for the GCM-driven GEM simulations for the current 1981–2010 and future 2071–2100 periods is shown in Fig. 4, along with the change of dew point depression which is defined by the difference between the daily mean air temperature and dew point temperature. In general, two types of changes are noted for future climate; a shift in the P–T curve to the right as for MRTMS or an extension of the P–T curve to the right as for WCOAST, WCRDRA, NPLAINS, NWFOR, NEFOR, YUKON, MACK, and EARCT in both two GEM simulations. For GRTLKS, both changes are noted depending on the lateral boundary condition, i.e. driving GCM. The above discussed changes indicate possible increase of extreme precipitation at higher temperatures in future climate. This increase is more dominant for RCP8.5 than RCP4.5 scenario. The peak-like structure of the P–T relationship for the inland regions is also noted in future climate, but with the breaking point shifted to the right by about $2\text{--}3^{\circ}\text{C}$ compared to that for current climate. This shift in the breaking point indicates that constant relative humidity can be maintained up to a relatively high temperature in the future.

Looking in detail at the projected changes to the P–T relationship, the future P–T slopes for GEM_MPI are closer to linear at CC or sub-CC scalings until the breaking point for WCRDRA, NPLAINS, and NEFOR regions, compared to GEM_Can. This suggests that GEM_MPI simulates relatively higher increases in moisture available to extreme precipitation at CC scaling rate for these regions. However, the projected changes to the simulated P–T slope vary depending on the climatic region and simulation. For example, the opposite result is noted for WCOAST. The GEM_Can, in general, projects more

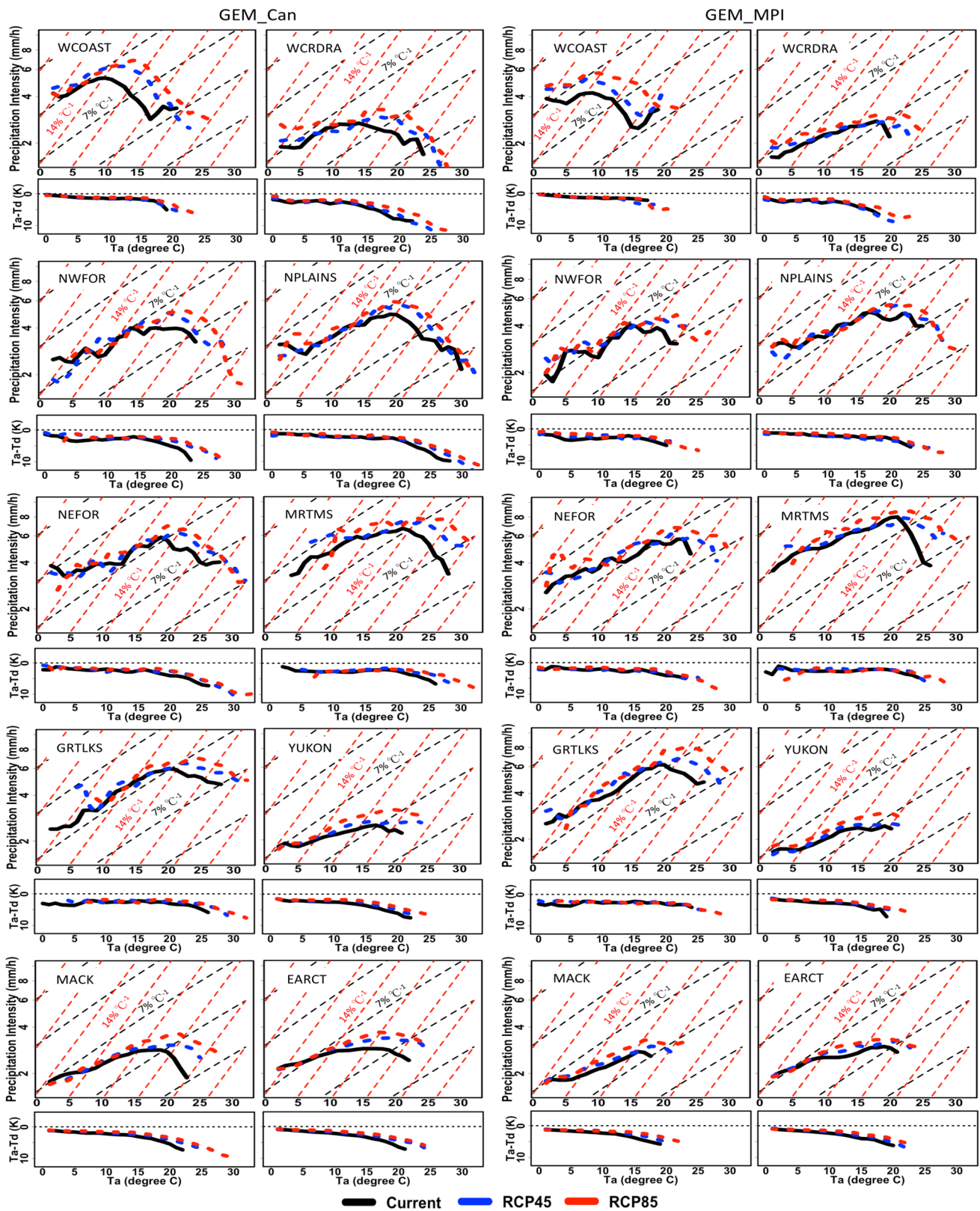


Fig. 4 Model simulated 95th percentile of precipitation intensity—daily mean air temperature relation for 1 h duration for the current 1981–2010 and future 2071–2100 periods for RCP4.5 and 8.5 scenarios, respectively.

Bottom panel of each sub-plot shows the dew point depression which is defined by the difference between the temperature (T_a) and dew point temperature (T_d)

extreme precipitation events than the GEM_MPI after the breaking point, particularly for inland regions and the RCP8.5 scenario. This can be attributed to the higher temperature increases in GEM_Can for this region compared to GEM_MPI.

The spatial pattern of the precipitation scaling rates ($\%/^{\circ}\text{C}$) for 1 h duration for the future 2071–2100 period and the relative change (%) of P–T slopes between future and current 1981–2010 periods are analyzed in Fig. 5 at the observation points shown in Fig. 1. Higher precipitation scaling rates continue to be the case for inland regions compared to coastal regions in future climate. However, the relative changes to the P–T slope do not exhibit any clear pattern. For example, the P–T slopes for most of the locations in the northern part of WCOAST are projected to decrease by up to 40%, regardless of the scenario and lateral boundary condition. The southern area of WCOAST, however, shows the opposite result, except for the GEM_MPI for the RCP4.5 scenario. As a result, the change of the area-averaged P–T slope for the WCOAST is not clear due to the offsetting effect induced by opposite changes depending on the sub-region, as shown in Fig. 4. NPLANS and GRTLKS show relatively higher P–T slopes in future climate, with slight variation in magnitude between the GEM_Can and GEM_MPI simulations, in particular for the RCP8.5 scenario. For the other regions, both increases and decreases in the P–T slope are noted at observation points, but the changes are not statistically significant (see Fig. 5). Precipitation-dew point temperature relationship is mostly similar to that of precipitation-daily air temperature. Some climatic regions, such as NWFOR, project opposite trends, unlike daily air temperature, but they are not statistically significant.

Figure 6 shows the spatial distribution of the 95th percentile of precipitation intensity for 1 h duration for different temperature bins. As expected, for the temperature bins from 5 to 20 °C for the current 1981–2010 period, the precipitation intensities generally increase with temperature though the precipitation area shrinks. The maximum precipitation intensities for the NWFOR, NPLAINS, MRTMS, GRTLKS, and some parts of NEFOR and EARCT (WCOAST, WCRDRA, YUKON, and MACK) occur in the 15–20 °C (10–15 °C) temperature bins. For temperature bins higher than 20 °C, some differences can be noted between GEM_Can and GEM_MPI simulations. GEM_Can has a relatively larger precipitation area with 3–5 mm/h from the NWFOR to MRTMS, while the GEM_MPI precipitation area is confined to smaller parts of NEFOR and GRTLKS. This pattern can be partly explained by the different temperature biases inherited from the driving data (Diro and Sushama 2017). GEM_Can and GEM_MPI simulations have warm and cold biases, respectively, of about 1–4 °C over Canada, compared to observations. Therefore, the opposite temperature biases may induce the difference in precipitation

simulation and this discrepancy seems to be dominant at high-temperature bins.

For the future 2071–2100 period, the precipitation intensity and area increase for all bins, particularly over southeastern Canada for the high-temperature bins. The precipitation areas expand to the north for all temperature bins compared to the current 1981–2010 period and these extensions are more dominant for RCP8.5 scenario. In addition, the precipitation increases for the 15–25 °C temperature bins are more significant around the southeastern area and the shifts in the breaking points from the 15–20 °C to 20–25 °C temperature bins are found in this region. For the temperature bins above 25 °C, significant expansion of precipitation area is found for the NWFOR to MRTMS, in particular for GEM_Can simulation for RCP8.5 scenario. The GEM_MPI simulations also project some increases in the precipitation area for the temperature bins above 25 °C. However, this is relatively small compared to GEM_Can simulations. This can be explained by the relatively lower temperature increases in GEM_MPI in the late 21st century compared to GEM_Can simulation (Diro and Sushama 2017).

The spatial patterns of convective precipitation contribution to total 3 hourly extreme precipitation is analyzed in Fig. 7. Considering the model configuration where convective precipitation is set to be output every 3 h, the convective precipitation contribution is estimated from 3 hourly total and convective precipitations. Generally, the spatial patterns of the 95th percentile of total precipitation intensities for various temperature bins for 3 h duration are similar to those for 1 h duration in current and future periods (Fig. S3 in the supplementary material). The contribution of convective precipitation to total precipitation is larger for the high-temperature bins. However, the mountainous regions show large contributions of convective precipitation due to the orographic effect even in the low-temperature bins. In future climate, the contribution of convective precipitation in the low-temperature bins is generally expected to decrease. This is related to the relatively lower frequency of extreme precipitation events in the low-temperature bins due to the overall mean temperature increase in the future. For temperature bins higher than 15 °C, the extended precipitation areas in future climate see up to 80% convective precipitation contribution. This contribution is more distinct in GEM_Can, which projects relatively higher temperature increases in future climate, compared to GEM_MPI.

The spatial distribution of the dew point depression (°C) and Convective Available Potential Energy (CAPE, J/kg) corresponding to short-duration precipitation extremes for the current 1981–2010 and future 2071–2100 periods are shown in Figs. 8 and 9, respectively. The CAPE was calculated from the simulated daily values at all pressure levels in order to compare the dew point depression. The dew point depression for temperature bins up to 15 °C has lower values,

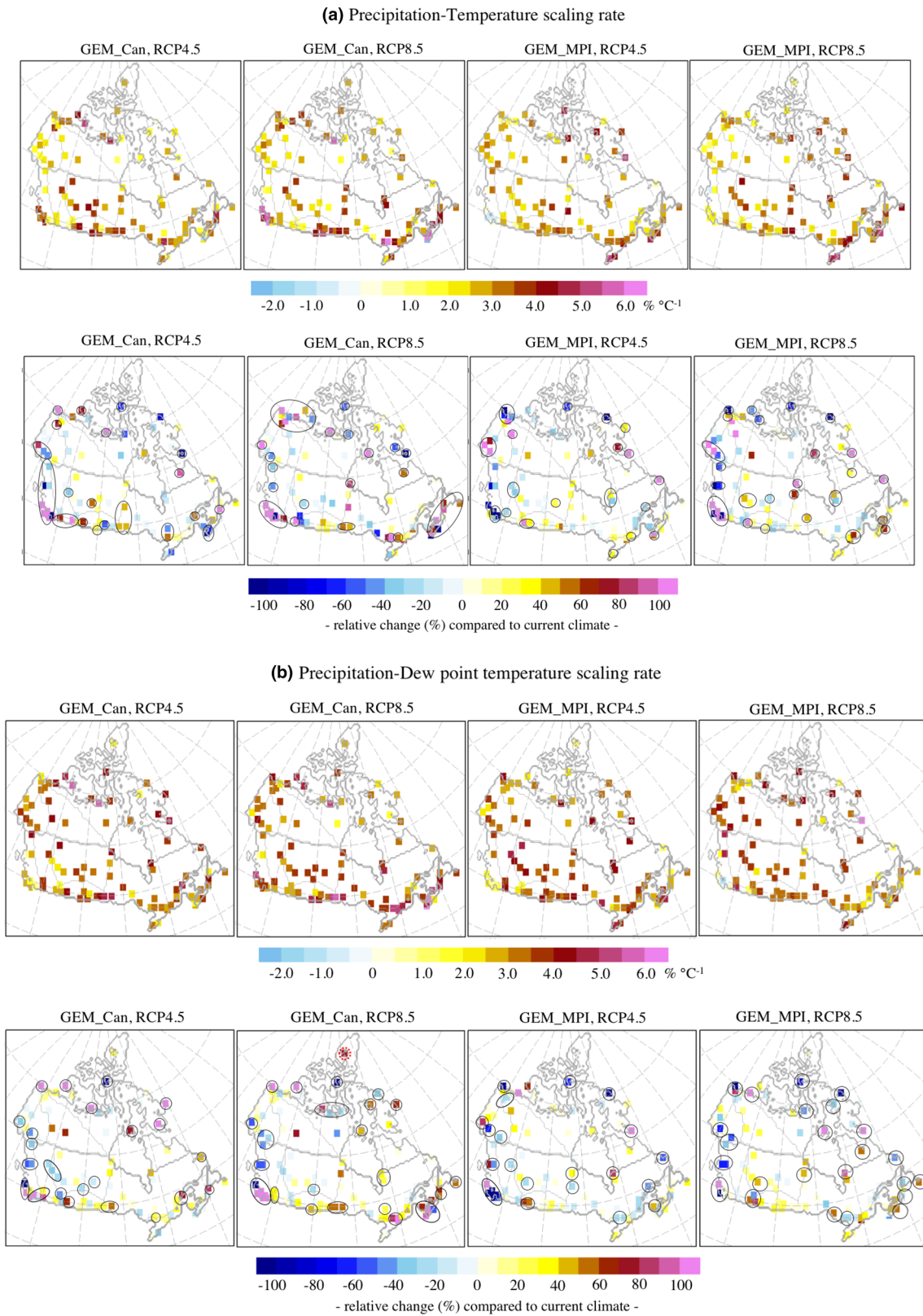


Fig. 5 Same as Fig. 3 but for GEM simulations for the future 2071–2100 period for RCP4.5 and 8.5 scenarios. Relative change (%) of the P–T slopes in the future period with respect to the current 1981–2010

period is also shown in the second row of **a** and **b**. The dots within the black circle indicate points with statistically significant changes at the 5% significance level of t test

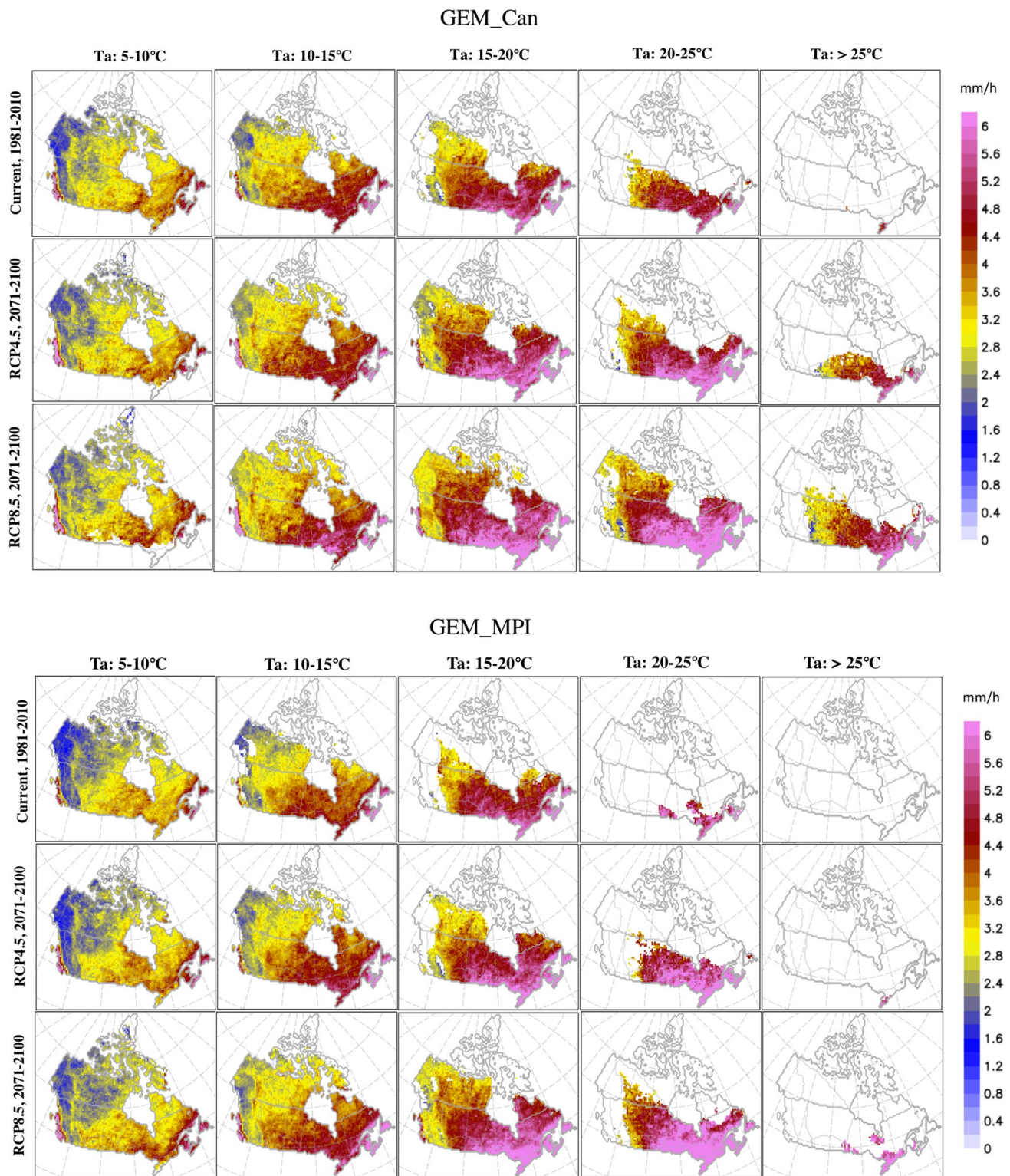


Fig. 6 Spatial distribution of GEM simulated 95th percentile of precipitation intensity of 1 h duration for different daily mean air temperature bins for the current 1981–2010 and future 2071–2100 periods for RCP4.5 and 8.5 scenarios

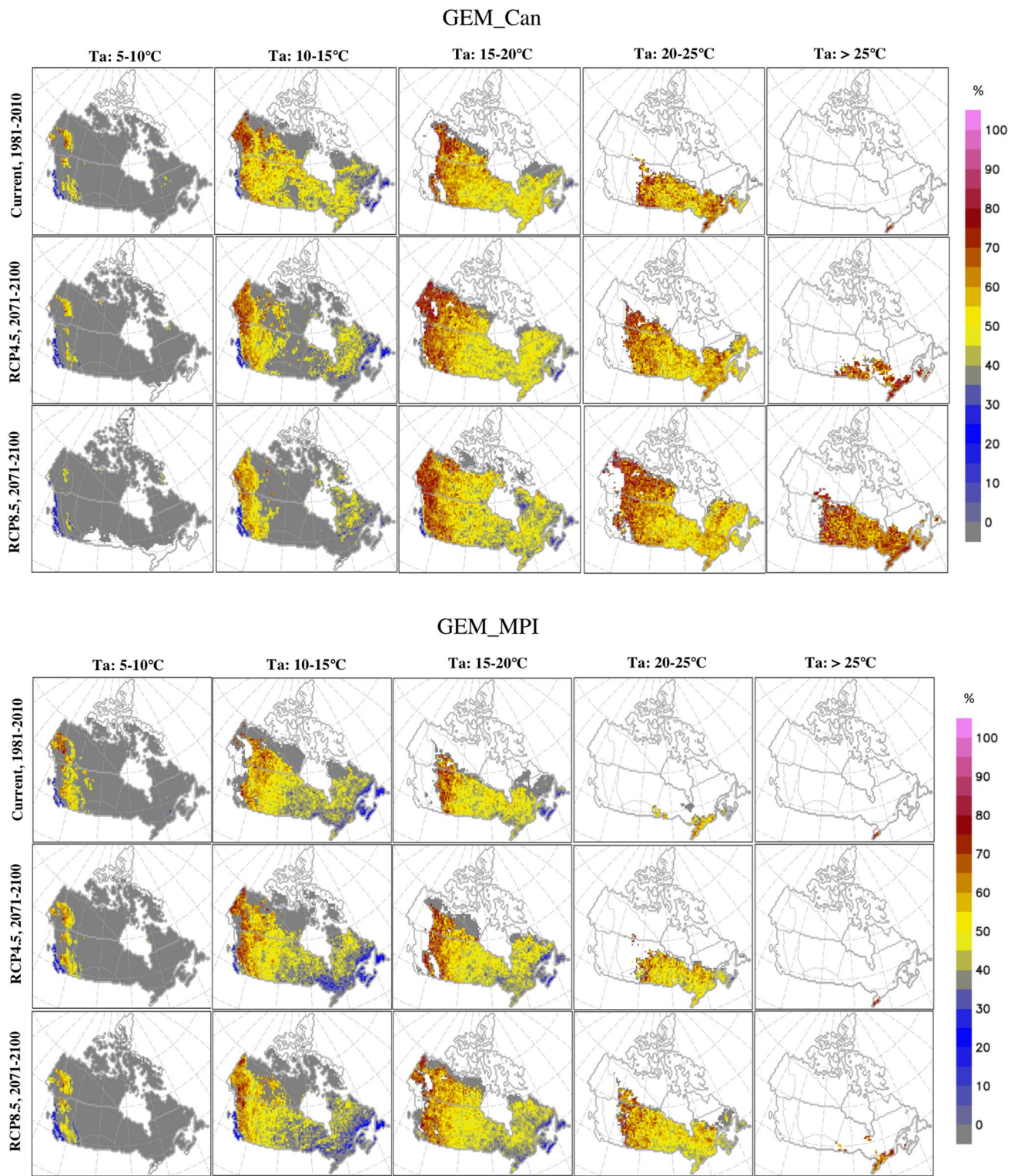


Fig. 7 Same as Fig. 6 but for convective precipitation contribution to the 95th percentile of precipitation intensity for 3 h duration. The grey shading indicates regions with precipitation for the various bins

suggesting near saturation condition. Relatively lower CAPE values also appear in these temperature bins. Therefore, precipitation in the low-temperature bins is largely due to high

relative humidity. However, the precipitation intensity is relatively low than in the high-temperature bins due to the limitation of atmosphere water-holding capacity (Fig. 6).

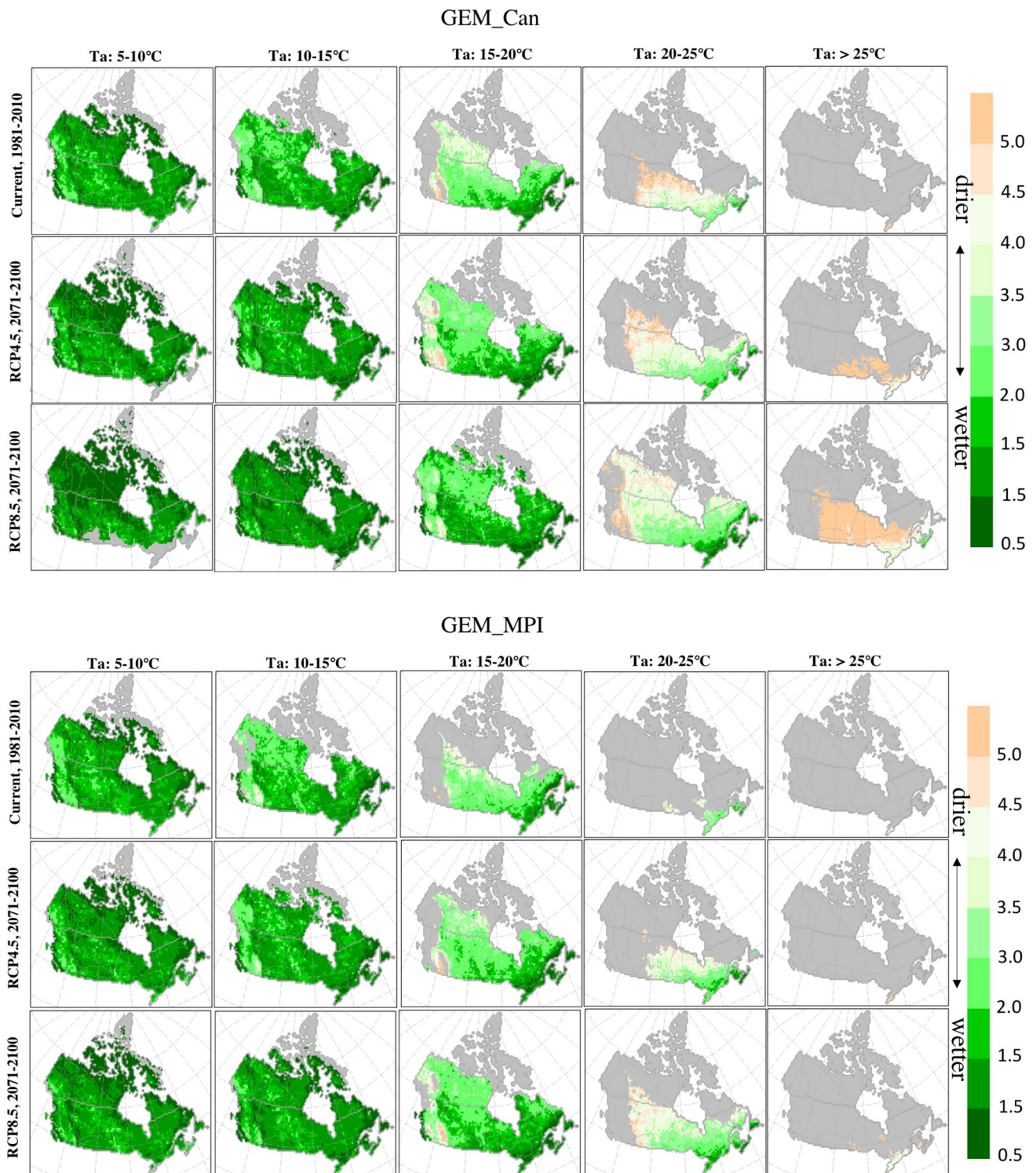


Fig. 8 Same as Fig. 6 but for dew point depression (°C) for the day when the 95th percentile of precipitation intensity for 3 h duration occurs

The future dew point depressions in temperature bins lower than 15 °C projected by GEM_Can are relatively lower than those by GEM_MPI, particularly for northern Canada and the RCP8.5 scenario. This indicates that GEM_Can projects

a moister atmosphere in future climate than current climate, compared to GEM_MPI. This can be partly explained by the fact that the relatively higher temperature increase projected by GEM_Can in future climate leads to increased

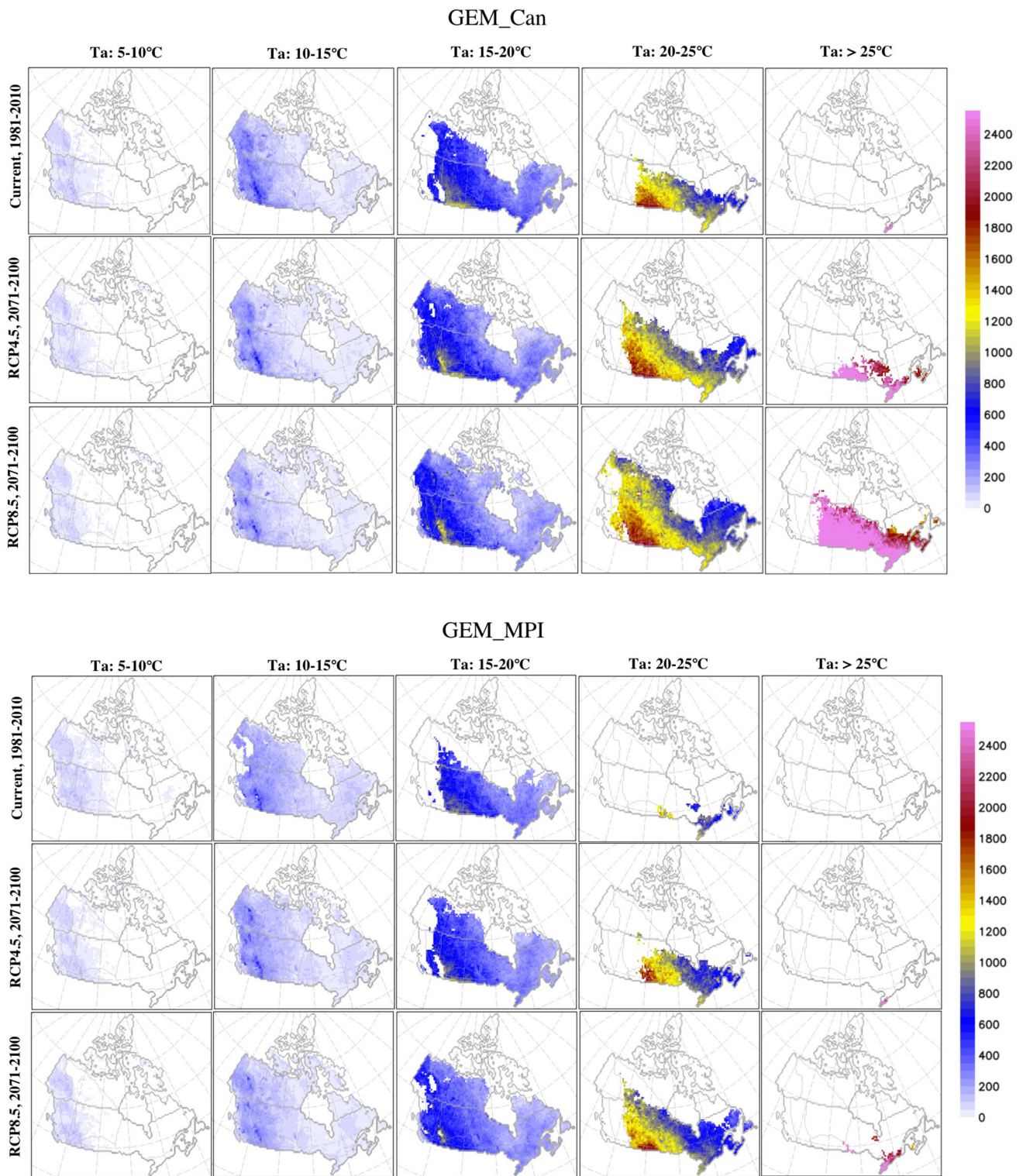


Fig. 9 Same as Fig. 6 but for convective available potential energy (CAPE, J/kg) for the day when the 95th percentile of precipitation intensity for 3 h duration occurs

evaporation, and consequently increases in near-surface moisture. Both the dew point depression and CAPE increase for the temperature bins above 15 °C, implying decreasing

relative humidity near surface, but strong convection due to the atmospheric instability brought by surface warming. These general features are also found in the result based on

the 99th percentile (figure not shown). This confirms again that the relative humidity gradually decreases with temperature increase beyond the breaking point (e.g., Lenderink and van Meijgaard 2010; Prein et al. 2016). An increase of P–T scaling is generally noted for the southeastern regions of Canada where CAPE increases are relatively pronounced (Fig. 5). This implies that both the statistical effect, which involves the transition of precipitation types from large-scale to convective rainfall events (e.g., Haerter and Berg 2009; Westra et al. 2014), and the physical effect, by which the convective process itself can overcome the thermodynamic limitation (Panthou et al. 2014; Park and Min 2017), are more robust in the precipitation-temperature relationship for future climate.

The relationship between CAPE and dew point depression for each climatic region is investigated in Fig. 10. In general, despite the differences depending on the climatic region and simulation, non-linear positive relationships are found. The GEM_Can generally show a logarithmic relationship for in the 2–8 °C dew point depression range, followed by an exponential relationship above 8 °C for most climatic regions. The GEM_MPI also simulates a somewhat similar relationship in the NWFOR, NEFOR, and NPLAINS. However, exponential relationships are noted for the WCOAST, WCRDRA, MRTMS, and EARCT for all dew point depressions. Therefore, the complex dewpoint depression–CAPE relationships vary with climatic region and driving data, and further studies are needed to analyze them more thoroughly. In this study, as indicated in Fig. 10, these positive relationships in future climate are expected to have a similar structure to that in current climate but will be strengthened, in particular for the RCP8.5 scenario. This robust relationship between CAPE and dew point depression in future climate can be partly explained by the shift in breaking point towards higher temperatures due to the increase in both the surface air temperature and dew point temperature compared to the current climate.

5 Summary and conclusion

This study assesses characteristics of short-duration precipitation extremes in terms of the precipitation-temperature relationship in current and future climates for ten climatic regions of Canada. To achieve these goals, GCM-driven GEM simulations (GEM_Can, GEM_MPI) for the 120-year (1981–2100) period based on RCP4.5 and 8.5 scenarios are used. To evaluate the GEM simulations for the current 1981–2010 period, the observed and simulated hourly precipitation and temperature from the gauging stations of Environment Canada and GEM simulation driven by ERA-Interim reanalysis (GEM_ERA) are used. Climate change signals are obtained from the GEM_Can and GEM_MPI

simulations by comparing the future 2071–2100 period with the current 1981–2010 period.

In general, the observed P–T relationship is strongly influenced by precipitation duration and climatic region. For short durations (1–3 h), the P–T relationship with a peak-like structure is found for the inland regions. The P–T slopes decrease with duration for all regions. The P–T relationship (slopes) is not very sensitive to the percentiles (90th, 95th, and 99th) considered in this study. For the temperature bins between 12 °C and 18 °C for short-durations (1–3 h), super-CC (NPLAINS), CC (WCRDRA, NWFOR, NEFOR, MRTMS, GRTLKS, YUKON, MACK, and EARCT), and sub-CC (WCOAST) scalings are found. The GEM simulations capture the general regional features of P–T relationship over Canada where the sub-CC and CC scaling with peak-like structure are observed for the coastal and inland regions, respectively. However, they tend to underestimate the breaking point of temperature by about 3–5 °C compared to observations. This means that the decrease of relative humidity simulated by GEM starts at a lower temperature than observation. However, GEM simulations can reproduce more robust relation between short-duration precipitation extremes and dew point temperature, similar to the observation.

Two types of changes to the P–T relationship are noted for future climate depending on the climatic region. The P–T curve gets shifted to the right as for MRTMS or the P–T curve gets extended to the right as for WCOAST, WCRDRA, NPLAINS, YUKON, MACK, and EARCT. For NWFOR, NEFOR, and GRTLKS, both changes are noted depending on the lateral boundary condition. The changes are more clear for RCP8.5 than RCP4.5 scenario. The breaking point generally is shifted to the right by about 2–3 °C compared to that for current climate and is collocated with the temperature at which dew point depression start to increase, indicating that constant relative humidity can be maintained up to a relatively higher temperature in the future.

Detailed analysis of short-duration precipitation extremes at bin-level demonstrates clearly the changing relative importance of relative humidity and CAPE for low to high temperature bins. Short-duration precipitation extremes in the low-temperature bins are largely due to high relative humidity, while strong convection due to the atmospheric instability brought by surface warming is largely responsible for short-duration precipitation extremes in the high temperature bins. The convective precipitation contribution to total precipitation is therefore higher for high temperature bins and lower for low temperature bins. In addition, increases in convective precipitation can lead to increases in soil moisture, which increases atmospheric moisture by evaporation, partly explaining why constant relative humidity is maintained up to higher temperatures. However, further studies should be conducted to understand this mechanism in detail.

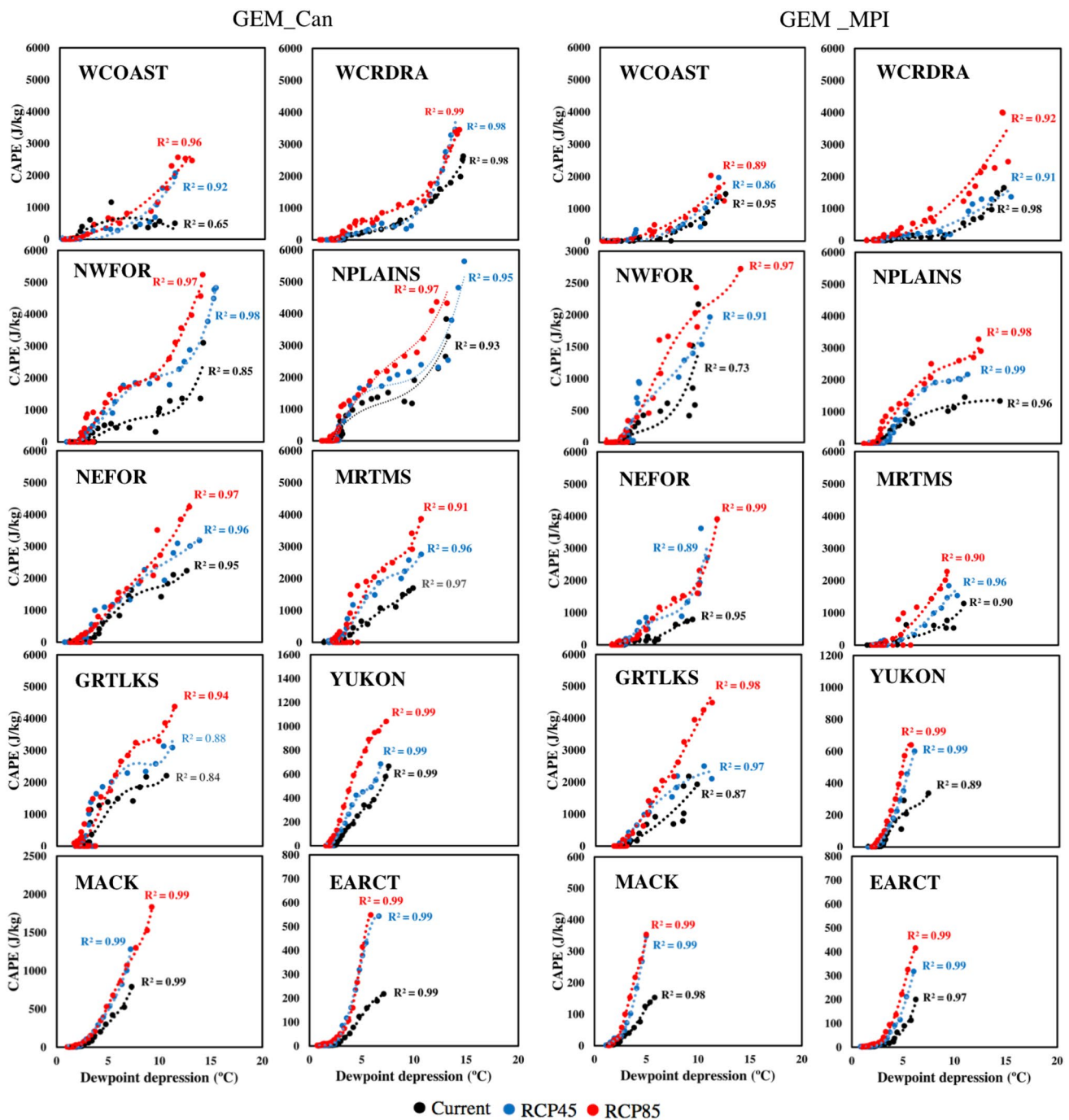


Fig. 10 Relationship between convective available potential energy (CAPE, J/kg) and dew point depression (°C) for the climatic regions of Canada for the current 1981–2010 and future 2071–2100 periods for RCP4.5 and 8.5 scenarios. The y-axis scales for CAPE are differ-

ent depending on the climatic regions. Third and fourth-degree polynomial curve regression fittings are used to estimate R^2 depending on the climatic region

This study provides useful insights regarding short-duration precipitation extremes for different climatic regions of Canada. However, regional climate model simulations used in this study are run at spatial resolutions of 50 km and rely on a convection parameterization scheme to compute the estimated average effects of convection over model grid

squares. Recent studies have proven that high-resolution convection-permitting simulations can further improve the magnitude and scaling rate of short-duration precipitation extremes due to better representation of the mesoscale dynamics and orographic effects (e.g., Prein et al. 2015, 2017; Kendon et al. 2017; Cannon and Innocenti 2019; Diro

and Sushama 2019). Thus, to utilize more realistic information in the fields such as civil engineering, convection-permitting simulations will be required to develop projected changes to short-duration precipitation extremes. In addition, an ensemble study using various regional and global climate models can help quantify uncertainties and thus provide more objective information for various applications.

Acknowledgements This research was funded by the Natural Sciences and Engineering Research Council of Canada and the Trottier Institute for Sustainability in Engineering and Design. The GEM simulations considered in this study were performed on the supercomputer managed by Compute Canada and Calcul Québec.

References

- Adamowski J, Adamowski K, Bougadis J (2010) Influence of trend on short duration design storms. *Water Resour Manag* 24:401–413
- Arora V et al (2011) Carbon emission limits required to satisfy future representative concentration pathways of greenhouse gases. *Geophys Res Lett* 38:L05805. <https://doi.org/10.1029/2010GL046270>
- Bao A, Sherwood JSC, Alexander LV, Evans JP (2017) Future increase in extreme precipitation exceed observed scaling rates. *Nature Clim Change*. <https://doi.org/10.1038/NCLIMATE3201>
- Bélair S, Mailhot J, Girard C, Vaillancourt P (2005) Boundary layer and shallow cumulus clouds in a medium-range forecast of a large-scale weather system. *Mon Weather Rev* 133:1938–1960
- Benoit R, Cote J, Mailhot J (1989) Inclusion of a Tke boundary-layer parameterization in the Canadian regional finite-element model. *Mon Weather Rev* 117(8):1726–1750
- Berg P, Moseley C, Haeter JO (2013) Strong increase in convective precipitation in response to higher temperature. *Nat Geosci* 6:181–185
- Cannon AJ, Innocenti S (2019) Projected intensification of sub-daily and daily rainfall extremes in convection-permitting climate model simulations over North America: implications for future intensity-duration-frequency curves. *Nat Hazards Earth Syst Sci* 19:421–440
- Cote J, Gravel S, Methot A, Patoine A, Roch M, Staniforth A (1998) The operational CMC-MRB global environmental multiscale (GEM) model. Part I: design considerations and formulation. *Mon Weather Rev* 126(6):1373–1395
- Dee DP et al (2011) The ERA-Interim reanalysis: configuration and performance of the data assimilation system. *Q J R Meteorol Soc* 137(656):553–597
- Delage Y (1997) Parameterising sub-grid scale vertical transport in atmospheric models under statistically stable conditions. *Bound-Layer Meteorol* 82:23–48
- Diro GT, Sushama L (2017) The role of soil moisture-atmosphere interaction on future hot spells over North America as simulated by the Canadian regional climate model (CRCM5). *J Clim* 30:5041–5058
- Diro GT, Sushama L (2019) Simulating Canadian Arctic climate at convection-permitting resolution. *Atmosphere*. <https://doi.org/10.3390/atmos10080430>
- Giorgetta MA et al (2013) Climate and carbon cycle changes from 1850 to 2100 in MPI-ESM simulations for the coupled model inter-comparison project phase 5. *J Adv Model Earth Syst* 5:572–597
- Haeter JO, Berg P (2009) Unexpected rise in extreme precipitation caused by a shift in rain type? *Nat Geosci* 2:372–373
- Hogg WD, Hogg AR (2010) Historical trends in short duration rainfall in the Greater Toronto area. In: Report for the Toronto and region conservation authority. <http://trca.on.ca/dotAsset/105189.pdf>
- IPCC (2013) The physical science basis. In: Contribution of working group I to the fifth assessment report of the intergovernmental panel on climate change. Cambridge University Press, Cambridge, p 1535
- Jeong DI, Sushama L (2018) Rain-on-snow events over North America based on two Canadian regional climate models. *Clim Dyn* 50:303–316
- Kain JS, Fritsch JM (1992) The role of the convective “trigger function” in numerical forecasts of mesoscale convective system. *Meteorol Atmos Phys* 49:93–106
- Kendon EJ, Ban N, Roberts NM, Fowler HJ, Roberts MJ, Chan SC, Evans JP, Fosse G, Wilkinson JM (2017) Do convection-permitting regional climate models improve projections of future precipitation changes? *Bull Am Meteorol Soc* 98:79–93
- Khaliq MN, Sushama L, Monette A, Wheaton H (2014) Seasonal and extreme precipitation characteristics for the watersheds of the Canadian Prairie Provinces as simulated by the NARCCAP multi-RCM ensemble. *Clim Dyn*. <https://doi.org/10.1007/s00382-014-2235-0>
- Kim G, Cha D-H et al (2018) Future change in extreme precipitation indices over Korea. *Int J Climatol* 2018:e862–e874
- Lenderink G, van Meijgaard E (2008) Increase in hourly precipitation extremes beyond expectations from temperature change. *Nat Geosci* 1:511–514
- Lenderink G, van Meijgaard E (2010) Linking increases in hourly precipitation extremes to atmospheric temperature and moisture changes. *Environ Res Lett* 5:025208. <https://doi.org/10.1088/1748-9326/5/2/025208>
- Li J, Barker HW (2005) A radiation algorithm with correlated-k distribution. Part I: local thermal equilibrium. *J Atmos Sci* 62(2):286–309
- Martynov AR, Laprise L, Sushama K, Winger L, Separovic, Dugas B (2013) Reanalysis-driven climate simulation over CORDEX North America domain using the Canadian regional climate model, version 5: model performance evaluation. *Clim Dyn*. <https://doi.org/10.1007/s00382-013-1778-9>
- Mekis E, Donaldson N, Reid J, Zucconi A, Hoover J, Li Q, Nitu R, Melo S (2018) An overview of surface-based precipitation observation at Environment and Climate Change Canada. *Atmos Ocean* 56(2):71–95
- Miao C, Sun Q, Borthwick AGL, Duan Q (2016) Linkage between hourly precipitation events and atmospheric temperature changes over China during the warm season. *Sci Rep*. <https://doi.org/10.1038/srep22543>
- Mladjic B, Sushama L, Khaliq MN, Laprise R, Caya D, Roy R (2011) Canadian RCM projected changes to extreme precipitation characteristics over Canada. *J Clim* 24:2565–2584
- Muller CJ, O’Gorman PA, Back LE (2011) Intensification of precipitation extremes with warming in a cloud resolving model. *J Clim* 24:2784–2800
- Oh SG, Suh MS (2018) Changes in seasonal and diurnal precipitation types during summer over South Korea in the late twenty-first century (2081–2100) projected by the RegCM4.0 based on four RCP scenarios. *Clim Dyn* 51:3041–3060
- Panthou G, Mailhot A, Laurence E, Talbot G (2014) Relationship between surface temperature and extreme rainfalls: a multi-time scale and event-based analysis. *J Hydrometeorol* 15:1999–2011
- Park IH, Min SK (2017) Role of convective precipitation in the relationship between subdaily extreme precipitation and temperature. *J Clim* 30:9527–9537
- Plummer DA et al (2006) Climate and climate change over North America as simulated by the Canadian RCM. *J Clim* 19:3112–3132
- Prein AF, Langhans W, Fosse G, Ferrone A, Ban N, Goergen K, Keller M, Tolle M, Gutjahr O, Feser F, Brisson E, Kollet S, Schmidli J, van Lipzig NPM, Leung R (2015) A review on regional

- convection-permitting climate modeling: demonstrations, prospects, and challenges. *Rev Geophys* 53:323–361
- Prein AF, Rasmussen RM, Ikeda K, Liu C, Clark MP (2016) The future intensification of hourly precipitation extremes. *Nature Clim Change*. <https://doi.org/10.1038/NCLIMATE3168>
- Prein AF, Liu C, Ikeda K, Bullock R, Rasmussen RM, Holland GJ, Clark M (2017) Simulating North American mesoscale convective systems with a convection-permitting climate model. *Clim Dyn*. <https://doi.org/10.1007/s00382-017-3993-2>
- Romps DM (2011) Response of tropical precipitation to global warming. *J Atmos Sci* 68:123–138
- Schroeder K, Kirchengast G (2018) Sensitivity of extreme precipitation to temperature: the variability of scaling factors from a regional to local perspective. *Clim Dyn* 50:3981–3994
- Shaw SB, Royen AA, Riha SJ (2011) The relationship between extreme hourly precipitation and surface temperature in different hydroclimatic regions of the United States. *J Hydrometeorol* 12:319–325
- Shephard MW, Mekis E, Morris RJ, Feng Y, Zhang X, Kilcup K, Fleetwood R (2014) Trends in Canadian short-duration extreme rainfall: including an intensity-duration-frequency perspective. *Atmos Ocean* 5:398–417
- Shuttleworth WJ (1993) Evaporation. In: Maidment DR (ed) *Handbook of hydrology*, chap. 4. McGraw-Hill, New York, USA, pp 4.1–4.53
- Sundqvist H, Berge E, Kristjánsson JE (1989) Condensation and cloud parameterization studies with a mesoscale numerical weather prediction model. *Mon Weather Rev* 117(8):1641–1657
- Teufel BGT et al (2017) Investigation of the 2013 Alberta flood from weather and climate perspectives. *Clim Dyn* 48:2881–2899
- United Nations (2017) *World population prospects: the 2017 revision, key findings and advanced tables*. Department of Economic and Social Affairs, Population Division, United Nations Press, p 47
- Verseghy DL (2009) CLASS-The Canadian land surface scheme (version 3.4)-technical documentation (version 1.1). In: Internal report, Climate Research Division, Science and Technology Branch, Environment Canada, p 183
- Westra S, Fowler HJ, Evans JP, Alexander LV, Berg P, Johnson F, Kendon EJ, Lenderink G, Roberts NM (2014) Future changes to the intensity and frequency of short-duration extreme rainfall. *Rev Geophys* 52:522–555
- Woodhams BJ, Birch CE, Marsham JH, Bain CL, Roberts NM, Boyd DFA (2018) What is the added value of a convection-permitting model for forecasting extreme rainfall over tropical East Africa. *Mon Weather Rev* 146:2757–2780
- Yeh KS, Cote J, Gravel S, Methot A, Patoine A, Roch M, Staniforth A (2002) The CMC-MRB global environmental multiscale (GEM) model. Part III: nonhydrostatic formulation. *Mon Weather Rev* 130(2):339–356
- Zadra A, McTaggart-Cowan R, Roch M (2012) Recent changes to the orographic blocking. In: Seminar presentation, PRN, Dorval, Canada, 30 March 2012. http://collaboration.cmc.ec.gc.ca/science/rpn/SEM/dossiers/2012/seminaires/2012-03-30/Seminar_2012-03-30_Ayrton-Zadra.pdf. Accessed 27 Aug 2018
- Zhang X, Zwiers FW, Li G, Wan H, Cannon AJ (2017) Complexity in estimating past and future extreme short-duration rainfall. *Nat Geosci*. <https://doi.org/10.1038/NNGEO2911>

Publisher's Note Springer Nature remains neutral with regard to jurisdictional claims in published maps and institutional affiliations.